Planar velocity measurements of the gas and liquid phase in dense sprays by flow tagging

S. Krüger and G. Grünefeld

University of Bielefeld, Faculty of Physics
Postfach 100131, 33501 Bielefeld, Germany
Tel. 49-521-1065442, Fax. 49-521-1062958.
E-mail: gruenefe@physik.uni-bielefeld.de

S. Arndt

Robert Bosch GmbH
FVSLE-Sh, Postfach 106050, 70049 Stuttgart, Germany

W. Hentschel

Volkswagen AG
1785-EZLP, 38436 Wolfsburg, Germany

ABSTRACT

We report on measurements of the gas and liquid phase velocity in *dense* automotive direct injection sprays by 2D laser-based flow tagging. Velocity measurements in dense sprays are generally difficult with conventional techniques because of the high number densities of droplets, the optical thickness of the medium, and multiple light scattering effects. The present flow tagging experiments are based on luminescent molecules which are used as the flow tracer. Flow tagging of the liquid phase is performed by exciting phosphorescence of the tracer molecules by a grid of pulsed write laser beams. The gas phase is tagged by inducing photodissociation of a suitable parent molecule using the write laser grid. The motion of the gas phase is probed by inducing fluorescence from one of the photogragments (NO) by using a read laser sheet. It is demonstrated that instantaneous and mean velocity fields can be measured in this way. This leads to conclusions on the interaction of continuous and dispersed phases in dense sprays.

1. INTRODUCTION

The interaction of gas and liquid phase plays an important role for secondary break-up and evaporation of sprays (Faeth, 1983, Sirignano, 1993). The relative (slip) velocity of gas and liquid phase is a major parameter in these processes. The slip velocity can be determined from the velocity fields of gas and liquid phase. It is demonstrated in this work that gas and liquid phase velocity measurements can be performed in *dense* sprays by using 2D laser-based flow tagging techniques. Velocity measurements in *dense* sprays, such as automotive direct injection (DI) gasoline and Diesel sprays, are generally difficult with conventional techniques because of the high number densities of droplets, the optical thickness of the medium, multiple light scattering effects, and sometimes strong out-of-plane motion (Le Coz, 1998, Araneo and Tropea, 1999, Zhao et al., 1999, Hentschel et al., 1999). Phase Doppler Anemometry (PDA) also suffers from beam steering effects in high-temperature environments. Particle image velocimetry (PIV) is often not possible because the images become blurred due to multiple scattering, so that individual particles can not be resolved. This holds for measurements in the gas and liquid phase as well (Adrian, 1986, Hassan et al., 1993, Sridhar and Katz, 1995). It should be noted that dense sprays are technically important. For example, high-pressure swirl injectors, generating dense hollow-cone sprays, are currently being developed for automotive direct injection spark ignition engines (Fraidl et al., 1996, Zhao et al., 1999, Hentschel et al., 1999).

For these reasons, flow tagging techniques based on molecular tracers have been developed and applied to dense sprays at the University of Bielefeld (Krüger and Grünefeld, 2000a&b). We prefer *molecular* tracers because it is well known that a number of problems arise from seed particles, such as particle lag and disturbance of the flow field. Previous flow tagging experiments, which are based on molecules or particles, are discussed elsewhere (Boedecker, 1989, Falco and Chu, 1987, Finke and Grünefeld, 2000, Hiller et al., 1984, Miles et al., 1987, Wehrmeyer et al., 1999). To our knowledge the first applications of laser flow tagging techniques to sprays have been described in prior papers (Krüger and Grünefeld, 2000a&b). These techniques are discussed in more detail and further results are given in the present paper.

Most of the laser flow tagging techniques described in the literature require two laser pulses, i.e., write and read lasers. They are based either on formation of tracer molecules by photodissociation (write process) and subsequent interrogation of a photofragment or the remaining parent molecules (read process) or molecular pump (write) and probe (read) mechanisms (Boedecker, 1989, Krüger and Grünefeld, 1999, Finke and Grünefeld, 2000, Miles et al., 1987, Wehrmeyer et al., 1999). In contrast, flow tagging can also be performed by a single laser pulse when phosphorescent substances are used as the tracer (Falco and Chu, 1987, Hiller et al., 1984, Krüger and Grünefeld, 2000b). The spatial position of the laser-excited phosphorescent substances is recorded by a gated camera after being convected by the flow. The use of phosphorescent substances also allows performing multiple consecutive velocity measurements within the phosphorescence lifetime, for example, by using a multi-frame camera as the detector or by `droplet group tracking´. An example is given elsewhere (Krüger and Grünefeld, 2000b).

It was mentioned above that PDA and PIV encounter severe problems in dense sprays. In contrast, a flow tagging technique is hardly affected by multiple light scattering when the distance and width of the tag lines are wide enough so that they can still be resolved. Beam attenuation does not affect the feasibility of the technique, as long as the tag lines are recognized. Laser beam steering is not an important factor because the spatial positions of the write laser beams can be recorded. Therefore, flow tagging can be performed in dense sprays. It should also be noted that strong out-of-plane motion is not problematic in most flow tagging experiments. Thus, it is possible to do the measurements, for example, in dense *swirling* sprays. It is also noteworthy that the three velocity components in a plane can be measured by stereoscopic flow tagging (Krüger and Grünefeld, 1999).

2. EXPERIMENTAL

2.1 Spray

Initial measurements have been performed in a hollow-cone gasoline direct injection spray. The prototype swirl injector and electronics were supplied by S. Arndt (Robert Bosch GmbH, Stuttgart). It has been operated with 50bar rail pressure in room air. Ethanol has been used as the fuel. The measurements have been performed at 1ms after triggering the injector, i.e., in the fully developed spray pulse (pulse length: 1.5ms). The maximum droplet density is about $5 \cdot 10^6/cm^3$ in the probe volume. The Sauter mean diameter of the droplets is $d_{32} \sim 15 \mu m$ (thus, the average droplet spacing at maximum density is $\sim 4 d_{32}$). This spray is comparable to previously investigated sprays, in which PIV measurements have proved to be difficult (Hentschel et al., 1999).

2.2 Gas-phase velocity measurements

Flow tagging of the gas phase is performed in this work by using two consecutive laser pulses, as mentioned above. The

present set-up is outlined in Fig. 1a), but the detector is not shown. An image-intensified CCD camera is employed as the detector. A Mie scattering image from the central plane of the spray is included in Fig. 1 to demonstrate the field of view and the orientation of the spray. The field of view (32mm x 24mm) has been imaged onto the CCD camera by using a spherical focussing mirror (f=35cm, d=25cm, aluminum). A well defined tracer molecule distribution is generated by a write laser grid via photodissociation of parent molecules, which are present throughout the probe volume. The tracer molecules are convected with the flow. The read laser is fired after a certain delay Δt in order to probe the tracer molecules using laser-induced fluorescence (LIF). The read laser beam is formed to a thick sheet (10mm x 25mm) so that all the tracer molecules reside within the probe volume after being convected by the flow. Tert-butyl nitrite, $(CH_3)_3CONO$, is used as the parent molecule in the present experiment (Krüger and Grünefeld, 1999). Seeding of gaseous tert-butyl nitrite (~1% mole fraction) is performed by a low velocity coflow of nitrogen as shown in Fig. 1a). The tracer gas is predominantly drawn into the spray by the entrainment gas flow. The velocity of the coflow is orders of magnitude smaller than the gas velocities in the spray, so that it does not significantly disturb the gas flow within the spray. A 248-nm KrF excimer laser is used as the write laser. The photodissociation cross-section of tert-butyl nitrite is about $10^{-18}cm^2$ at 248nm. Two sets of write laser lines, each ~0.5mm in diameter (~10mJ/pulse), are created by splitting and focussing the beam of the dissociation laser, basically by using two arrays of 15 cylindrical lenses (f=30 cm). The photofragment probed by the read laser is NO, which is excited at about 226nm via the $R_{21}(17.5)$ line in the $\gamma(0,0)$ band system. A second tunable, narrowband KrF excimer laser is used for this purpose. The detection of NO and discrimination against Mie scattering is described in more detail in a prior paper (Krüger and Grünefeld, 1999). It should be noted that the tagging scheme based on tert-butyl nitrite yields the possibility to record instantaneous 2D velocity fields containing a large number of vectors, in contrast to most other tagging schemes, because a considerable number of tag lines can be created by a single commercial write laser, and NO can be probed effectively.
The initial tracer distribution (at t=0) must be recorded in particular in the case of laser beam steering. This is discussed in more detail elsewhere (Krüger and Grünefeld, 2000a). However, we determined the initial tracer distribution by probing NO using the read laser at $t \approx 0$. This is possible because the initial tracer distribution was found to be reproducible from pulse to pulse.

2.3 Droplet velocity measurements

The droplet tagging set-up is outlined in Fig. 1b), but the detector is again not shown. An image-intensified double-frame `progressive scan´ CCD camera (PCO Sensicam) is employed as the detector. It is capable of recording two images with a delay down to ~1µs. A Mie scattering image that has been recorded with a thin laser sheet in the central plane of the spray is included in Fig. 1b). It represents the distribution of the liquid phase in the central plane. The field of view (33mm x 44mm) has been imaged onto the CCD camera under right angles by using the same spherical focussing mirror that was used before.
The central plane of the spray is illuminated by a write laser grid as shown in Fig. 1b). A frequency-quadrupled (266nm) Nd:YAG laser (Spectra Physics) is used as the laser source. Two sets of write laser lines, each ~0.5mm x 2mm in diameter (70µJ/pulse), are created as described before. Droplet tagging is performed in this work by using phosphorescent molecules. A lanthanide chelate (Tb^{3+}-dipicolinic acid, Molecular Probes) dissolved in ethanol (10^{-3} M) is employed in the present experiment. The phosphorescence lifetime of the terbium chelate is roughly 1ms. It exhibits a broad absorption peak around 280nm. The phosphorescence occurs at two sharp peaks at 491nm and 545nm which are both collected by the camera system. Biacetyl is another interesting phosphorescent molecule that was previously used for flow tagging in the gas phase (Hiller et al., 1984). It may be used for flow tagging measurements in sprays as well,

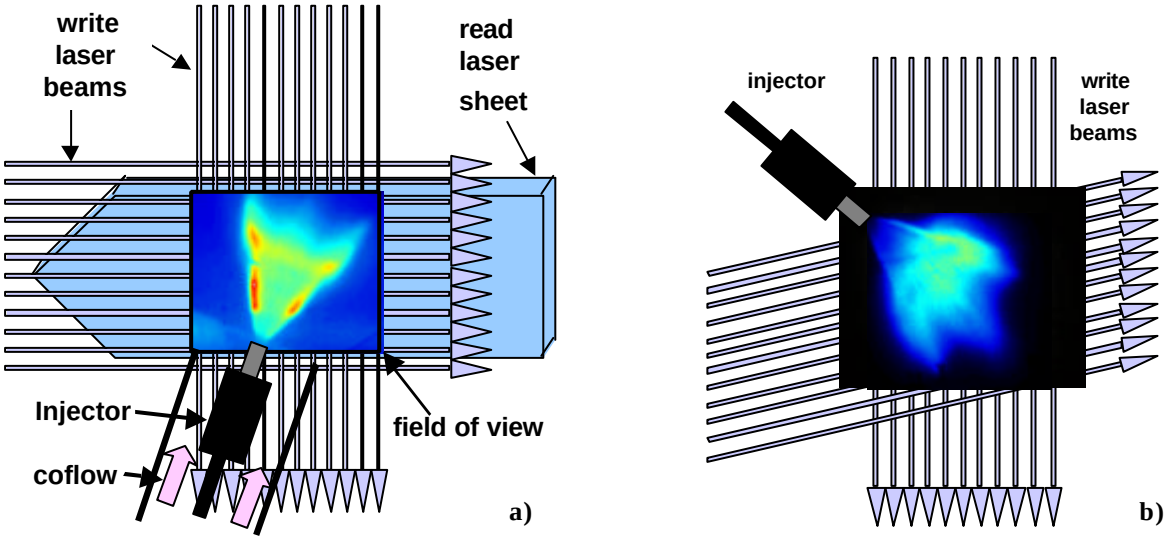

Figure 1. Experimental set-ups of gas-phase (a) and liquid-phase (b) velocity measurements. The intensified CCD cameras are not shown. Instead, Mie scattering images are included to show the spray at 1ms after triggering the injector.

which is discussed in detail elsewhere (Krüger and Grünefeld, 2000b).
The initial distribution of the excited molecules at t≈0 has been determined in each individual spray pulse by using the double-frame option of the CCD camera (see next Section). Thus, the technique is not affected by any possible beam steering.

3. RESULTS AND DISCUSSION

3.1 Gas-phase velocity measurements

Fig. 2 shows a pair of typical CCD images measured in the spray with a delay of $\Delta t=40\mu s$. Both images show LIF from NO and some residual Mie scattering. Fig. 2a) has been averaged over 10 measurements, and Fig. 2b) results from a single measurement It can be seen that there are considerable spatial variations of the NO signal on the grid, basically because of beam attenuation in the dense spray, but the grid is still recognized in Fig. 2b). The displacement field of the distorted grid in Fig. 2b) with regard to the initial grid in Fig. 2a) yields the instantaneous gas velocity field. The displacement is found by employing an optical flow algorithm (Tokumaru and Dimotakis, 1995, Grünefeld et al., 1999). The resulting instantaneous velocity field is given elsewhere (Krüger and Grünefeld, 2000a). It is very similar to the mean velocity field averaged over 10 instantaneous measurements, which is depicted in Fig. 3. The pulse-to-pulse fluctuations of the instantaneous velocity fields will be discussed in more detail below.
The optical flow algorithm yields continuous velocity fields. However, the true spatial resolution of the measurement technique is determined as follows. Each local velocity measurement is based on a certain fraction of the images, i.e., a so called interrogation spot, similar to most PIV techniques. The size of the interrogation spots determines the spatial resolution. It is clear that the determination of the velocity field is locally only possible along the gradients of the scalar image intensity $\tilde{N}I(\mathbf{x})$ (Tokumaru and Dimotakis, 1995). This so called `aperture problem´ sets a lower limit for the ultimate spatial resolution, because it is, essentially, necessary to find non-vanishing gradients in both directions, i.e., $\partial I(\mathbf{x})/\partial x \neq 0$ and $\partial I(\mathbf{x})/\partial y \neq 0$, respectively, in each interrogation spot. This is illustrated in Fig. 4. A small part of a single LIF (or phosphorescence) image at t=0 is depicted in Fig. 4a). The isointensity contour lines of the image intensity $I(\mathbf{x})$ are schematically shown in this figure. In addition, the position of the tag lines are given as broken lines (The image intensity $I(\mathbf{x})$ can be assumed to be maximal in most cases on the tag lines.) Each interrogation spot yields in an independent velocity measurement.

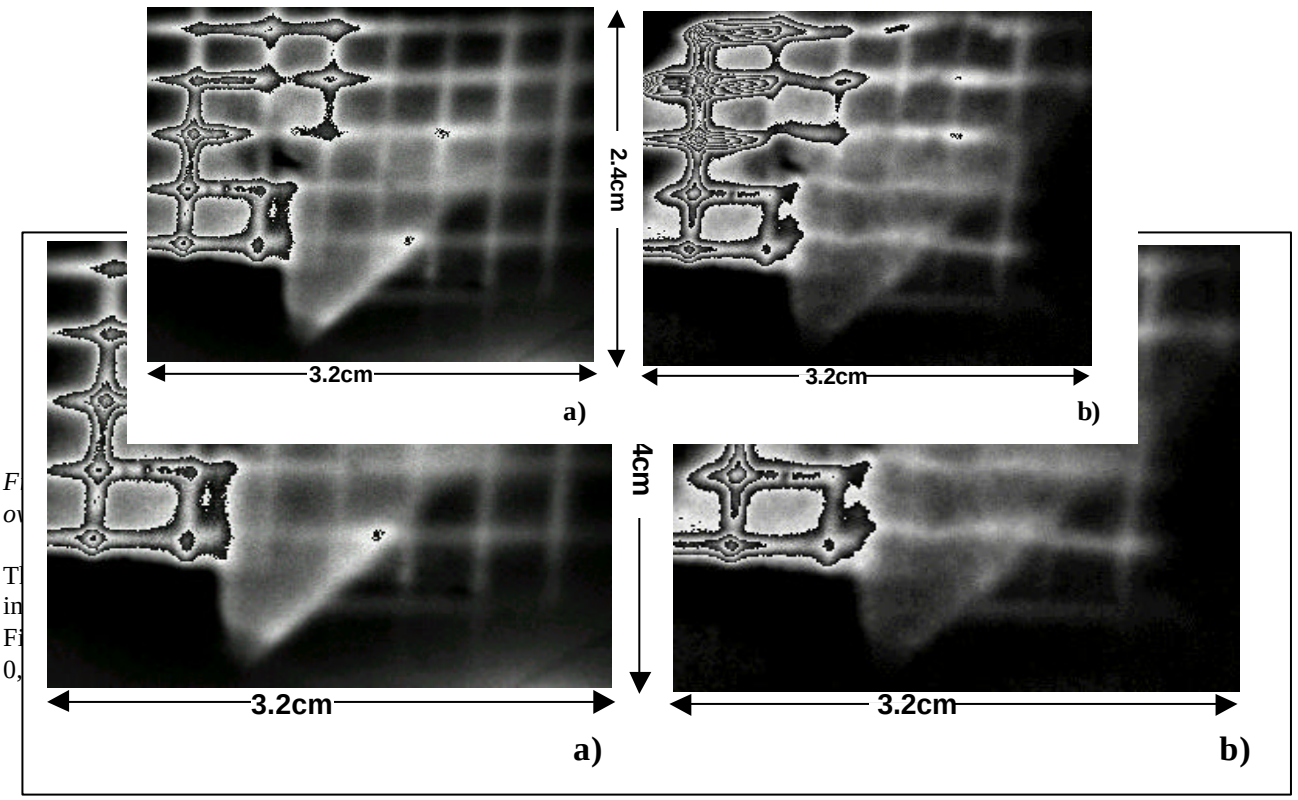

F
ov

T
in
Fi
0,

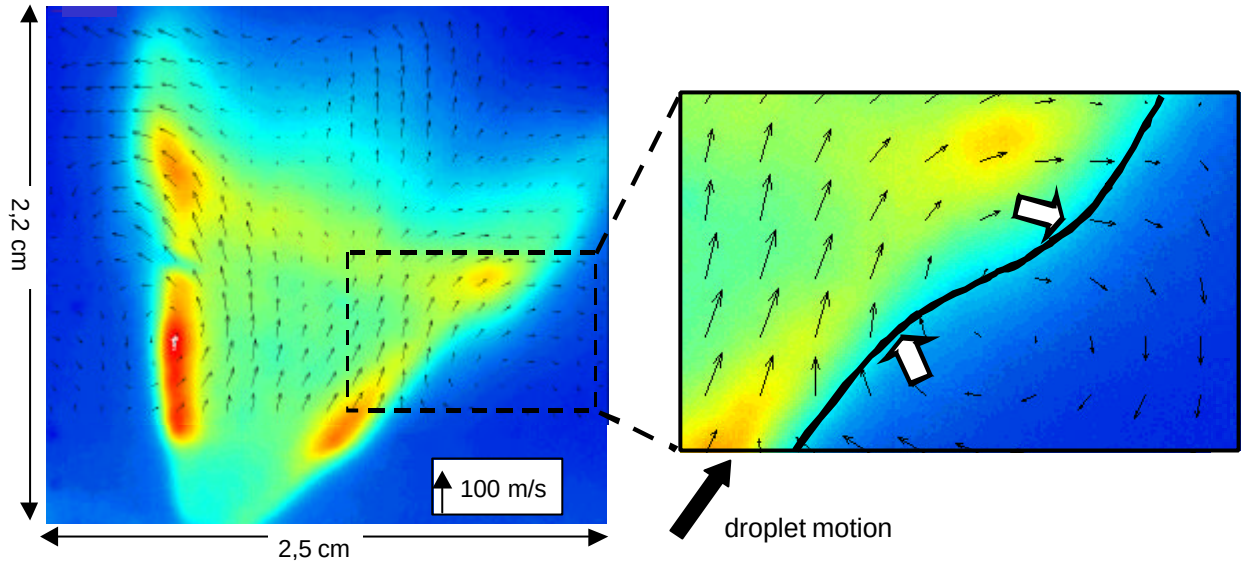

Figure 3. Mean velocity field (averaged over 10 instantaneous measurements) of the gas phase. A Mie scattering image is given in the background to show the distribution of the liquid phase. The edge of the spray cone has been highlighted by a thick line in the enlarged image on the right hand side. The large arrows indicate the principal motion of gas and liquid phase respectively

reduced. Thus, the ultimate spatial resolution of the tagging technique (without further assumptions) is essentially given by d_{min} = b / 2, where b is the tag line distance. This implies that the number of independent velocity vectors in an instantaneous measurement, n, is four times the number of tag line intersections. Thus, n equals 24 in the example of Fig. 4, and n equals 140 in the case of the real measurements with 5 x 7 tag lines. (There are about twice as many velocity vectors shown in Fig. 3, which have been computed, essentially, by interpolation).

The accuracy of the *instantaneous* measurements is basically limited by the displacement of the tag lines, $s=v\Delta t$, the width of the tag lines (full width at half maximum), ω, and the uncertainty to determine the center of the displaced tag

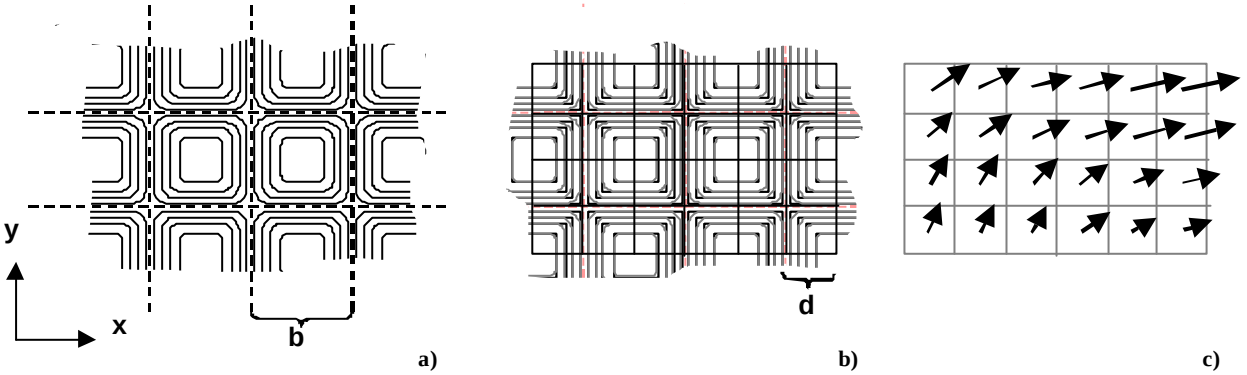

Figure 4. The spatial resolution of 2D flow tagging techniques. (a) Tag lines (broken) and isointensity contour lines of the image intensity. (b) Interrogation spots with size d. (c) Resulting field of independent velocity measurements (example).

lines, σ_s. The latter can be estimated to be 10-20% of ω in these initial measurements, where ω equals about 1mm. Two vertical image intensity profiles from a pair of raw (LIF) images (see Fig. 2) are given in Fig. 5 as an example. The accuracy of a typical velocity measurement with v=50m/s and Δt=40µs based on these images can be estimated as $\sigma_v/v \approx \sigma_s/s$ = 5-10%. This is illustrated in the enlarged profile on the right hand side of Fig. 5. Accordingly, smaller velocities exhibit larger errors. It should be noted that molecular diffusion does not significantly affect the accuracy in this application because of the short delay Δt=40µs. It is also clear that the accuracy of a mean velocity field is generally

better than the accuracy of the instantaneous velocity fields.
A Mie scattering image, similar to the one given in Fig. 1a), is shown in the background of Fig. 3 to indicate the spray contour. It can be seen that there are large eddies (up to ~60m/s) formed at the edge of the spray cone, and strong air entrainment is observed close to the nozzle. Obviously, these eddies deform the shape of the spray cone, although the droplets travel at high velocity (of the order of 50m/s, see below). This can be explained by the small size of the droplets, since d_{32}~15µm. The enlarged image on the right hand side of Fig. 3 demonstrates more clearly that the deformation of the spray cone is indeed correlated to the measured air flow.

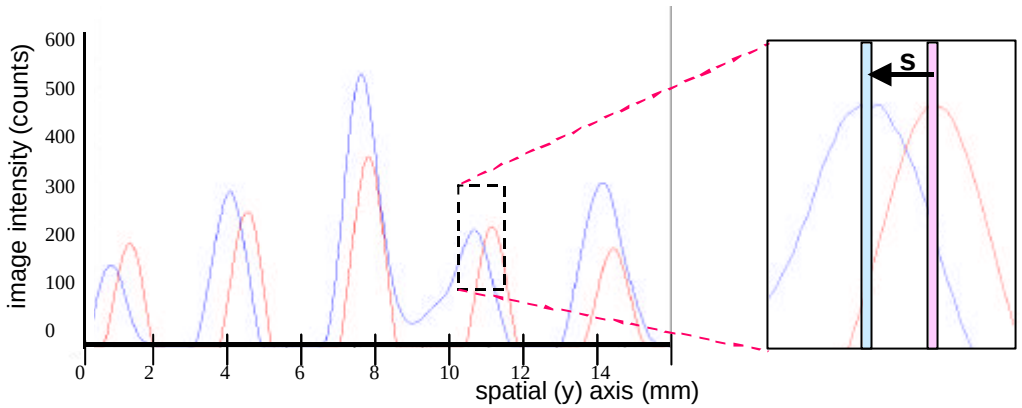

Figure 5. The accuracy of flow tagging measurements. Two typical vertical profiles from the center of two raw (LIF) images are given. The accuracy is determined by the uncertainty s_s (=width of the grey vertical bars on the right hand side) divided by the displacement s.

It was mentioned before that the pulse-to-pulse fluctuations of the gas flow are small. This can be seen in the standard deviation field of the velocity magnitudes, which is given elsewhere (Krüger and Grünefeld, 2000a). In particular, the pulse-to-pulse fluctuations of the gas flow are very small (20-30%) in most regions of the spray cone, where the droplet density is high (The fluctuations are much larger inside the hollow-cone and in the ambient air where the droplet density is low.) One might think that the high-pressure spray generates a highly turbulent flow field of the gas phase. However, this is not necessarily true, since small particles tend to reduce the turbulent intensity (Gore and Crowe, 1989, Hetsroni, 1989): Small particles follow the gas flow, and thereby turbulent energy is transformed into kinetic energy of the particles. In conclusion, the spray tends to generate high turbulence only in regions where the droplet density is relatively low.

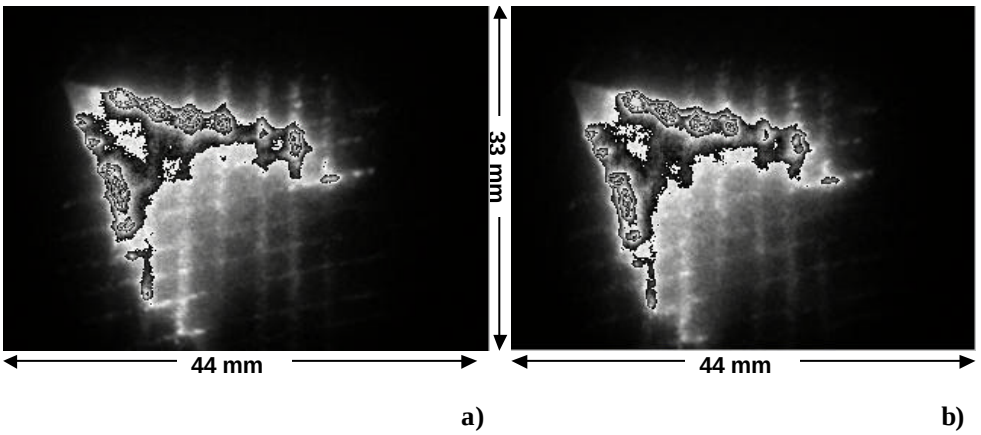

Figure 6. Pair of phosphorescence single-shot images recorded in a single spray pulse with a delay of Dt=15ms.

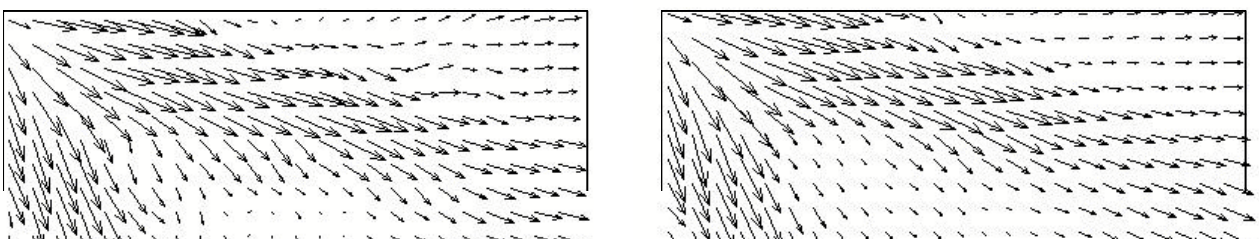

Figure 7. (a) Instantaneous droplet velocity field resulting from the image pair shown in Fig. 6. (b) Mean droplet velocity field computed from 20 instantaneous measurements.

3.2 Droplet velocity measurements

Fig. 6 shows a pair of typical phosphorescence single-shot images measured in the spray with a delay of Δt=15µs. Both images have been measured in an individual spray pulse using the double-frame camera described above. There is no

residual Mie scattering in these images because both have been recorded after the laser pulse. Fig. 6a) has been measured 1-6µs after the laser pulse, and Fig. 6b) has been measured at 16-21µs after the laser pulse (gate length: 5µs). The hollow-cone structure of the spray can be nicely seen in these images.

The displacement field of the distorted grid in Fig. 6b) with regard to the initial grid in Fig. 6a) yields the instantaneous droplet velocity field. Again the displacement is found by employing the optical flow algorithm mentioned above. The resulting instantaneous velocity field is given in Fig. 7a). In addition, a mean velocity field averaged over 20 instantaneous measurements is shown in Fig. 7b). Obviously, instantaneous and mean velocity fields are quite similar, in particular close to the edge of the hollow cone, where the droplet density is high (see below). This corresponds to low fluctuations of the gas velocity field in these regions. The maximum drop velocity found at the edge of the spray cone (mean velocity field) is ~90m/s. It is not surprising that much smaller drop velocities are found in regions where the droplet density is low. Overall, the apparent deceleration of the main droplet stream at the edge of the spray cone is relatively low, i.e., only ~30% across the field of view. This can be explained by the fact that the gas velocity is directed more or less parallel to the droplet motion in these regions and its magnitude is only 20-50% smaller than the droplet velocity (see Fig. 3).

Some details of the velocity field in Fig. 7b) can be observed more clearly in the corresponding velocity *magnitude* field which is given in Fig. 8a). In particular, the velocity distribution close to the edge of the hollow cone, i.e., in the droplet mainstream, is not as uniform or smooth as one might expect. There are at least two significant velocity peaks on both `branches´ in the droplet mainstream close to the nozzle (upper left quarter of Fig. 8a). However, this does not imply that the droplets were accelerated in some regions when they travel in the mainstream. Instead, it will be demonstrated in a forthcoming paper (based on acceleration measurements) that this velocity distribution is caused by unsteady effects.

The corresponding relative standard deviation of 20 instantaneous velocity measurements is given in Fig. 8b). It can be seen that the fluctuations are very low (5-10%) in the mainstream of the droplets as mentioned before. This implies that the relative error of the instantaneous measurements is also smaller than 5-10% at least in these regions. Much larger fluctuations are seen in regions where the droplet density is low. This is partly caused by larger measurement errors in these regions, in particular at the very edges of the images. It is not surprising that the signal-to-noise ratio is poor when the droplet density is very low (compare Fig. 6).

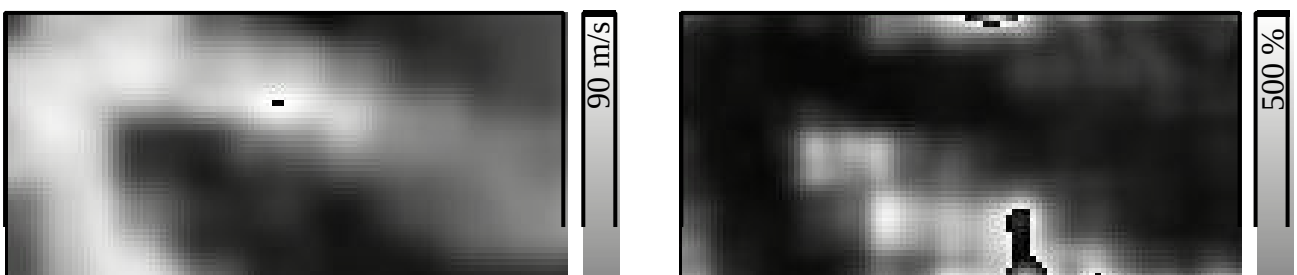

Figure 8. (a) Velocity magnitude field computed from the data in Fig. 7b). (b) Relative standard deviation of the velocity magnitudes from 20 instantaneous measurements

4 CONCLUSIONS

It is demonstrated that velocity fields of the gas and liquid phase can be measured in *dense* sprays by the present flow tagging methods. In comparison to well established techniques, such as PDA and PIV, the present techniques are much less affected by multiple light scattering, beam steering and beam attenuation in optically thick two-phase flows.
The present techniques yield the possibility to study the interactions of dispersed and continuous phase in highly particle-laden, evaporating and non-evaporating gas flows.
The measurement error of these initial instantaneous gas and droplet velocity fields can be estimated to be 5-10% (except in some regions of the droplet velocity fields, where the droplet density is low). It can be assumed that the accuracy of the mean velocity fields is better. In principle, it is possible to improve the accuracy of the instantaneous velocity fields up to a certain limit by using longer delays between the two measurements. The spatial resolution of the flow tagging measurements can be estimated to be half the spacing of the tag lines in a first approach. This is about 2mm in the gas velocity and 1.6mm in the droplet velocity measurements. This spatial resolution is sufficient to resolve the basic structures in these gas and liquid phase velocity fields. It is clear that the spatial resolution can be improved by using smaller spacing between the tag lines in other applications if necessary.
It is noteworthy that these flow tagging techniques can also be performed close to walls. Any stray light from walls can be suppressed by exploiting the wavelength shift of the luminescence and the time resolution in the case of the phosphorescence measurements. We have recently investigated the interaction of the dense spray with a wall by using the droplet tagging technique and this will be discussed in a forthcoming paper. Furthermore, it can be expected that these flow tagging techniques can be applied in high-pressure environments, for example, in internal combustion engines. Thus, it should be possible to study automotive direct injection sprays under more realistic operating conditions.

ACKNOWLEDGEMENTS

This work has been supported by the German Federal Ministry for Science and Education (BMBF) under contract No. 13N7181-0 and 13N7182-1.

REFERENCES

Adrian, R.J. (1986). „Multi-point optical measurement of simultaneous vectors in unsteady flow-a review“, Int. J. Heat & Fluid Flow 7(2), 127-145

Araneo, L., Tropea, C. (1999). in: Spray `99, (5. Workshop über Techniken der Fluidzerstäubung und Untersuchungen von Sprühvorgängen) Universität Bremen, in English

Boedecker, L.R. (1989). „Velocity measurement by H_2O photolysis and laser-induced fluorescence of OH“, Opt. Lett. 14 (10), 473-475

Faeth, G.M. (1983). „Evaporation and combustion of sprays“ Prog. Energy Combust. Sci. 9, 1-76

Falco, R.E., Chu, C.C. (1987). „Measurement of two-dimensional fluid dynamic quantities using a photochromic grid tracing technique“, *Proc. SPIE* Vol. 814, 706-710

Finke H., Grünefeld, G., (2000). „An Experimental Investigation of Extinction of Curved Laminar Hydrogen Diffusion Flames", *Proc. Combust. Inst.* 28, Symposium (International) on Combustion, Edinburgh

Fraidl, G.K., Piock, W.F., Wirth, M. (1996). „Gasoline direct injection: actual trends and future strategies for injection and combustion systems“ SAE Tech. Paper No. 960465

Gore, R.A. , Crowe, C.T. (1989). „Effect of particle size on modulating turbulent intensity“ Int. J. Multiphase Flow 15 (2), 279-285

Grünefeld, G., Finke, H., Bartelheimer, J., Krüger, S., „Probing the Velocity Fields of Gas and Liquid Phase Simultaneously in a Two-Phase Flow", Exp. in Fluids, in press (1999)

Hassan, Y.A., Philip, O.G., Schmidl, W.D. (1993). „Bubble Collapse Velocity Meaurements using a PIV Technqiue with Fluorescent Tracers", ASME FED-Vol. 172, 85-92

Hentschel, W., Homburg, A., Ohmstede, G., Müller, T., Grünefeld, G. (1999). „Investigation of Spray Formation of DI Gasoline Hollow-Cone Injectors in a Pressure Chamber and Glass Ring Engine by Multiple Optical Techniques" SAE Tech. Paper No. 1999-01-3660

Hetsroni, G. (1989). „Particles-Turbulence Interaction“, Int. J. Multiphase Flow 15 (5), 735-746

Hiller, B., Booman, R.A., Hassa, C., Hanson, R.K. (1984). „Velocity visualization in gas flows using laser-induced phosphorescence of biacetyl“ Rev. Sci. Instrum. 55 (12), 1964-1967

Krüger, S., Grünefeld, G. (1999). „Stereoscopic Flow Tagging Velocimetry", Appl. Phys. B 69, 509-512

Krüger, S., Grünefeld, G. (2000a). „Gas-Phase Velocity Field Measurements in Dense Sprays by Laser-Based Flow Tagging" Appl. Phys. B 70, 463-466

Krüger, S., Grünefeld, G. (2000b). „Droplet Velocity and Acceleration Measurements in Dense Sprays by Laser Flow Tagging“ submitted to Appl. Phys. B

Le-Coz, J.F. (1998). „Comparison of different drop sizing techniques on direct injection gasoline sprays“ Ninth Int. Symp. On Appl. Of Laser Techniques To Fluid Mechanics, Paper 7.3, Lisbon, Portugal

Miles, R.B., Cohen, C., Connors, J., Howard, P., Huang, S., Markowitz, E., Russell, G. (1987). „Velocity measurements by vibrational tagging and fluorescent probing of oxygen“ Opt. Lett. 12 (11), 861-863

Sirignano, W.A. (1993). „Fluid Dynamics of Sprays-1992 Freeman Scholar Lecture“ J. Fluids Engineering 115, 345-378

Sridhar, G., Katz, J. (1995). „Drag and Lift Forces on Microscopic Bubbles Entrained by a Vortex” Phys. Fluids 7, 389-399

P.T. Tokumaru, P.E. Dimotakis (1995). „Image Correlation Velocimetry“ Exp. in Fluids 19, 1-15

Wehrmeyer, J.A., Ribarov, L.A., Oguss, D.A., Batliwala, F., Pitz, R.W. (1999). „Flow tagging velocimetry for low and high temperature flowfields“ AIAA Paper 99-0646, 37th Aerospace Sciences Meeting & Exhibit, Jan. 11-14 Reno/NV

Zhao, F., Lai, M.-C., Harrington, D.L. (1999). „Automotive spark-ignited direct-injection gasoline engines“ Progr. Energy Combust. Sci. 25, 437-562